Storage and light scattering of microparticles in a ring-type electrodynamic trap

Al. A. Kolomenskii,[a] S. N. Jerebtsov, J. A. Stoker, M. O. Scully, and H. A. Schuessler
Department of Physics, Texas A&M University, College Station, Texas 77843-4242, USA

(Received 26 April 2007; accepted 10 September 2007; published online 1 November 2007)

We employ a Paul-Straubel ring-type electrodynamic trap for studies of single microparticles. Such a trap provides ready access for laser beams to a stored species and is especially suited for scattering and spectroscopic studies of fine particles. We derive the pseudopotential for such a trap and determine the stability regions for confinement of charged particles considering also the viscous force of a buffer medium and the force of gravity. The dynamics of microparticles in such a trap is numerically simulated. The diffraction pattern of light scattered on a polystyrene particle of about 10 μm diameter was registered. For measuring Raman spectra from a single dipicolinic acid microparticle, we used excitation at 488 nm and detection with a fiber optics spectrometer. To improve the collection of light, the trap with the stored particle was placed inside an elliptical mirror. © *2007 American Institute of Physics*. [DOI: 10.1063/1.2802287]

I. INTRODUCTION

The technique of electrodynamic traps was introduced by Paul and Steinwedel[1] (a mass spectrometer with a quadrupole trap) and as a mass filter by Paul and Raether.[2] The trap design based on an inhomogeneous electric rf field was used by Dehmelt for storage and spectroscopy of ions.[3] Straubel[4] modified Millikan's electrostatic balance[5] by adding an additional electrode providing an ac field and used this device to levitate and analyze microparticles. Different modifications of such a Paul-Straubel trap are of interest because of the strong localization of the field, enabling convenient study of single stored ions[6] and their simple electrode configuration allowing trap microfabrication.[7]

The necessity of analyzing small particles is encountered in different applications, for instance, such as detection and identification of aerosols,[8] studies of spectral properties of cells in biology,[9] and investigation of the particles formed as a result of chemical reactions.[10] Coulomb fission of evaporating charged droplets was investigated[11,12] and formation of Rayleigh jets was studied in detail.[13]

The technique of "optical tweezers" pioneered by Ashkin *et al.*[14] provides a possibility to work with neutral particles. Charged particles have an additional handle and can be levitated in electromagnetic fields.[4,15] Using levitation in suitable ac and dc fields, the characteristics of Rayleigh and Mie scattering[8,16] and Raman scattering[10,17,18] of microparticles were studied. While the elastic (Rayleigh and Mie) light scattering reflects mainly the size, shape, and complex refractive index of the particle, the measurements of the inelastic (Raman) scattering provide information on the chemical composition of the particle material, since the frequency shifts of the Raman peaks in the spectrum correspond to certain characteristic vibrational bands of the molecules.

We employ a simple ring-type trap similar to the one discussed in Ref. 6 for studying single microparticles. The trap consists of a ring electrode with an ac potential, and the potential at infinity is taken to be zero. In such a trap the gravitational force is compensated by an average electrical force which is not zero, since the particle spends more time in the region with a higher electric field. In this case the particle must oscillate to maintain a stationary state. When the ring is in the horizontal plane, the gravity force can be also balanced by the addition of two electrodes above and below the ring electrode with a dc potential applied to them, as was originally realized by Straubel,[4] and later a modified version was used by Kiefer *et al.*[18] The simple geometry of the trap allows obtaining explicit analytical formulas for the field in such a trap.[19] For a small particle moving in a gas environment (air), the viscous (drag) force of the medium becomes significant, as was first demonstrated by Millikan[20] and later thoroughly studied by Dahneke[21] and Lea and Loyalka.[22] In the atmosphere, the relative role of the drag force increases with the decrease of the size of a particle. The charge/mass ratio also tends to increase with the reduction of particle size. Therefore, much higher frequencies of the ac field are needed for trapping of very small particles, such as nanoparticles.

A detailed study of the unstable regions for axial confinement of a microparticle storage in a quadrupole trap (or as it was called in this case, an electrodynamic levitator) in the plane of (field strength parameter)-(drag coefficient) was carried out by Frickel *et al.*[23] and Davis.[24,25] We study the regions of stable trapping by taking also the viscosity and the force of gravity into account. We obtain unstable regions that combine instabilities for the axial and radial motions. From the theory of Mathieu functions[26] we identify also several regions exhibiting the highest stability for combined motion in both the radial and axial directions. It was shown[23] that the force of gravity leads to a phase shift between the particle motion in the vertical direction and the applied ac field. This phase shift was proposed to be used for "weighing" or size determination of a particle.[27] In this case, the electrodynamic trap plays a role of an electrodynamic balance that uses an ac

[a]Electronic mail: a-kolomenski@physics.tamu.edu

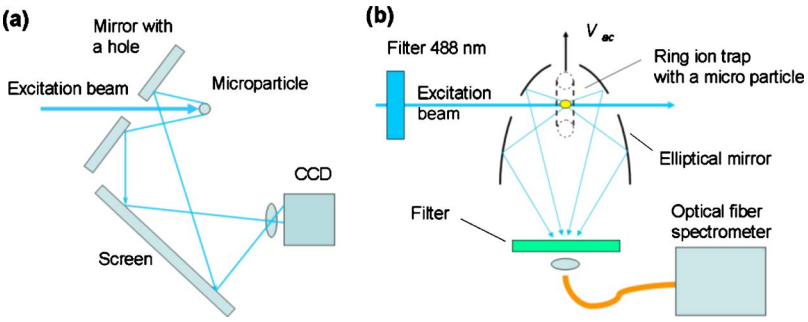

FIG. 1. (Color online) Experimental arrangements: (a) For observation of scattering diffraction patterns from microparticles and (b) for measurement of Raman scattering with an elliptical mirror and an optical fiber spectrometer.

field unlike the electrostatic balance of Millikan.[5] We calculate the oscillating motion of a trapped particle and demonstrate by direct numerical simulations the role of the viscous force in approaching the particle to the stationary state near the center of the trap. As an application of the trap, we characterize microparticles by both elastic and inelastic light scatterings. Such an approach is well suited for the identification of airborne particles, in particular, bacterial spores. We carried out measurements of light diffraction on a single ≈ 10 μm polystyrene particle and the Raman scattering from a ≈ 50 μm microparticle of a dipicolinic acid (DPA) powder stored in the trap. DPA together with its salts is a major constituent of bacterial spores.[28]

A particular feature of our setup used for Raman spectroscopic measurements is that the trap was placed inside an elliptical mirror, so that the light scattered from the particle positioned in one focus of the mirror could be collected from a large solid angle and detected in the other focus.

II. EXPERIMENTAL SETUP

An argon ion laser operating single line at 488 nm (Coherent, model CR-2000K) was used as the excitation light source. To eliminate weak emission plasma lines of the laser that had intensity comparable to the intensity of the Raman scattering, the output laser beam passed through a narrowband transmission interference filter centered at 488 nm with a full width at half maximum bandwidth of 10 nm. The trap consisted of a single ring with a radius $r=4$ mm. It was made of a copper wire of $r_w=0.45$ mm radius. Typically, an ac voltage of 0.3–1 kV and a frequency in the range of 100–1000 Hz were applied for the trapping of microparticles. The ring of the trap had a vertical orientation, convenient for light scattering experiments, and for Raman spectroscopic measurements it was inserted inside of an elliptical mirror that collected the scattered light from a large solid angle (about 10 sr).

For the observation of the backscattered light from a particle, we used a plane mirror with a small hole for transmission of the direct light [see Fig. 1(a)]. For measuring Raman spectra, the light collected by the elliptical mirror [Fig. 1(b)] passed through a filter that blocked the elastically scattered component (two Schott glass plates OG550, 2 mm thickness each) and was then focused on a tip of an optical fiber. The elliptical mirror provided an about 30-fold increase in the collection solid angle compared to the plane mirror geometry and had three openings: One for inserting the trap with the particle and two others for the entrance and exit of the laser beam (see Fig. 2). For stable particle storage, the elliptical mirror was grounded. The collected scattered light was guided by the optical fiber to a spectrometer (Ocean Optics 2000 with 25 μm entrance slit and a 1200 grooves/mm grating). A typical acquisition time was about 3 min. Resolution of the spectrometer was 20 cm^{-1}.

Polystyrene particles were 9.6 ± 1.9 μm in diameter (Duke Scientific Corp.). DPA powder was purchased from Sigma-Aldrich Corp. Microscopic studies of trapped DPA particles have shown that the typical size of the particles used for Raman measurements was about 30–50 μm. The spectra could be reproducibly obtained with the same trapped particles demonstrating that no noticeable changes in the sample occurred during the measurement.

III. TRAPPING OF MICROPARTICLES

A. Description of a charged particle in the trap

For description of trapping we consider a metal ring at an instantaneous potential of the form

$$V = V_{dc} - V_{ac} \cos \Omega t, \tag{1}$$

where V_{dc} is a constant potential measured relative to infinity and V_{ac} is the amplitude of the oscillating contribution. Assuming that X is the axis of symmetry of the ring of the trap, we obtain the following expressions for the components of the electric force near the center of the trap:

$$F_x = \frac{2q_0V}{z_0^2}x, \quad F_y = -\frac{q_0V}{z_0^2}y, \quad F_z = -\frac{q_0V}{z_0^2}z, \tag{2}$$

where $z_0=[2\ln(r_1/r_w)/\pi]^{0.5}r_1$ (for the derivation see Appendix). One can see that if F_y and F_z provide a restoring force, which is opposite to the displacement (if charges on the ring and the particle have equal signs), then F_x has the same sign as the displacement and is pushing the particle away from the trap. This is a reflection of Earnshaw's theorem, which

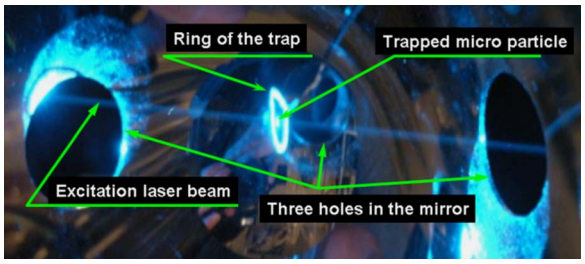

FIG. 2. (Color online) A view of the trap with stored DPA particle that were placed inside an elliptical mirror for measurements of Raman scattering.

states that a collection of freely moving charges cannot be maintained in a stable stationary equilibrium configuration solely by electrostatic forces. From Eq. (2), we find the expression for the hyperbolic electric potential in the vicinity of the trap center,

$$U(x,y,z) = (V_{dc} - V_{ac}\cos\Omega t)[x^2 - (y^2+z^2)/2]/z_0^2. \quad (3)$$

For simulations of the confinement of particles in the trap, we assumed that the charged particle is a sphere with a radius r_0 and introduced the Stokes' viscous force $F_v = -6\pi r_0 \eta v$, where η is the viscosity of the medium surrounding the trap and v is the velocity of the particle. In addition, the force of gravity $F_g = mg$ (m is the mass of the particle) was also taken into account. The equations of motion for the displacement $\boldsymbol{R} = \{x,y,z\}$ of the particle with mass m relative to the center of the ring is then $m\ddot{\boldsymbol{R}} = \boldsymbol{F} - Kr_0\dot{\boldsymbol{R}} - m\boldsymbol{g}$, where r_0 is the particle radius and the damping coefficient is $K = 6\pi\eta$ for a spherical particle (some more general cases and corrections to the Stokes' formula are considered in Ref. 21). This equation can be written in components in the following form:

$$\ddot{x} + 2p_x\dot{x} + (a_x - 2q_x\cos 2\tau)x = 0,$$

$$\ddot{y} + 2p_r\dot{y} + (a_r - 2q_r\cos 2\tau)y = 0, \quad (4)$$

$$\ddot{z} + 2p_r\dot{z} + (a_r - 2q_r\cos 2\tau)z + h = 0,$$

where the derivatives are taken over the dimensionless variable $\tau = \Omega t/2$, t is time, and the following dimensionless parameters are introduced: $p_x = p_r = p = (Kr_0/m\Omega)$, $a_x = -2a_r = (8q_0V_{dc}/mz_0^2\Omega^2)$, $q_x = -2q_r = (4q_0V_{ac}/mz_0^2\Omega^2)$, and $h = 4g/\Omega^2$.

The analysis of a particle motion can be simplified by presenting it as consisting of two components: The first one, called the secular or macromotion, is an averaged motion of the particle, and the second component, labeled the driving or micromotion, is an oscillating motion with the frequency of the external field. Using equations for the motion in a quickly oscillating field,[3,29] we obtain the effective potential for a secular (macro) motion of a charged particle

$$U_{eff} = \frac{1}{m\Omega^2}\left(\frac{2q_0V_{ac}}{z_0^2}\right)^2\left[x^2 + \frac{1}{4}(y^2+z^2)\right]. \quad (5)$$

B. Regions of stable trapping for microparticles: Nonzero viscous force and zero force of gravity

We operated the trap at $V_{dc}=0$, therefore, $a_x = -2a_r = 0$. Let us assume for now that the force of gravity can be neglected, $h=0$. It was shown that, when the viscous force is nonzero, the substitutions $x = \exp(-p\tau)x'$, $y = \exp(-p\tau)y'$, and $z = \exp(-p\tau)z'$ lead to the Mathieu equations with a modified parameters $a_x' = a_x - p^2$ and $a_r' = a_r - p^2$.[23,26] When the solution $\{x', y', z'\}$ has finite amplitude for $\tau -> \infty$ in some regions of the q-a plane, the actual coordinates $\{x,y,z\}$ of the particle displacement from the center approach zero as $\propto\exp(-p\tau)$. These regions correspond to the highest stability of the solutions of the original Eq. (4). They can be determined as an overlap of stable regions of the Mathieu equations (Ref. 26)

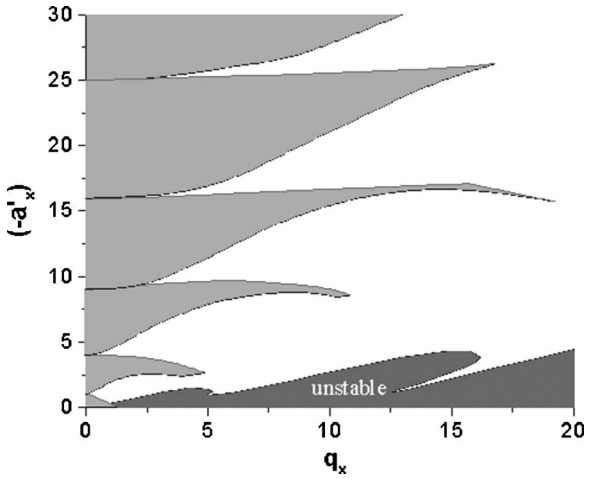

FIG. 3. The diagram shows several regions of highest stability (adjacent to the $-a_x'$ axis) and an unstable region (the area adjacent to the q_x axis).

for x and y (or z), in which a_x and a_r are substituted by $a_x' = a_r' = -p^2$. When $V_{dc}=0$ ($a_x=0$), the first five stability regions and a portion of the sixth are shown in Fig. 3 and correspond to the gray shaded area adjacent to the $-a_x'$ axis. The white areas are also stable; however, the convergence rate to zero of the solution $\{x,y,z\}$ reduces when moving away from the $-a_x'$ axis.

When no dc voltage is applied, $a_x' = a_r' = -p^2$. With the reduction of the particle size the value of $p^2 \propto r^{-4}$ quickly increases, so that both parameters a_x' and a_r' become negative numbers with a large absolute value, which means that trapping takes place at higher values along the $-a_x'$ axis on the diagram of Fig. 3. On the same q-a plane, an area exists that corresponds to unstable behavior of solutions of Eq. (4). For one of Eqs. (4), the unstable zones were determined in Refs. 23 and 24. Since an unstable behavior of any of the solutions of Eqs. (4) renders the particle motion unstable, the combination of unstable zones for all Eqs. (4) determines the region of unstable motion, which is shown in Fig. 3 as a dark shaded area adjacent to the q_x axis.

C. Trapping of microparticles: A zero viscous force and a nonzero force of gravity

For $V_{dc}=0$ and $p=0$, we have $a_x'=0$ and the stability diagram in the q_x-a_x plane shows[30] (see also Fig. 3) that the stable trapping takes place for $q_x \leqslant 0.908$, or using the definition of q_x, we find

$$q_0/m \leqslant 0.227 z_0^2\Omega^2/V_{ac}. \quad (6)$$

The condition of Eq. (6) can be presented in a different form. When a potential V is used for charging a spherical particle the charge on the particle is proportional to the applied voltage and the electrical capacitance of the particle, C. For a spherical particle we assume $C = 4\pi\varepsilon\varepsilon_0 r_0$ and the mass of the particle $m = (4/3)\pi r_0^3\rho_m$, where ρ_m is the density of the particle substance. Consequently, $q_0/m = (3V\varepsilon\varepsilon_0/\rho_m r_0^2)$ and from Eq. (6) we obtain the following condition:

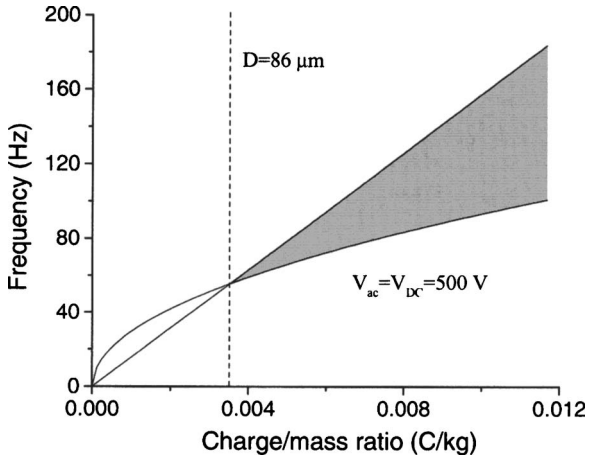

FIG. 4. The diagram showing the region of stable trapping as the shaded area, which is determined by the conditions of Eqs. (6) and (8) and extends to the right, to higher values of f and q_0/m (only part of this region within the presented range of parameters is shown). It was assumed that the particle was charged up to a potential $V=500$ V and the potentials on the ring were $V_{dc}=0$ and $V_{ac}=500$ V. The point of the intersection of the two border lines corresponds to a particle of maximum diameter that can be trapped (in this case, $d=86$ μm).

$$\varepsilon\varepsilon_0\left(\frac{V_0}{r_0}\right)\left(\frac{V_{ac}}{z_0}\right) \leqslant 3(fr)(fz_0)\rho_m, \tag{7}$$

where $f=\Omega/(2\pi)$. The left and right sides of this expression have dimension of the density of the electric and mechanical energy correspondingly.

In the presence of the gravitational force, for stationary behavior of a charged particle in the trap, another condition must is imposed. To enable the storage of a particle near the center of the trap, the force of gravity must be much weaker than the maximum force that can be provided by the pseudopotential. Consequently, the condition that the gravitational force only slightly perturbs confinement of the particle can be written in the form of the following inequality:

$$\frac{\partial}{\partial z_1}U_{\text{eff}} \sim \frac{1}{m\Omega^2}\frac{(2q_0V_{ac})^2}{z_0^3} \gg mg. \tag{8}$$

Assuming $V_{dc}=0$, $V_{ac}=V=500$ V, and for the values of parameters of the trap used in our experiments ($r_1=4$ mm, $r_w=0.45$), we can present the region, where the constrains of Eqs. (6) and (8) are fulfilled on a [frequency, $f=\Omega/(2\pi)$]-[charge/mass, q_0/m] diagram (see Fig. 4), as a shaded area. The point of the intersection of the border lines for the two conditions corresponds to a particle of maximum diameter that satisfies the above conditions. In the shaded area, the lower border line described by a square-root dependence $\propto(q_0/m)^{0.5}$ corresponding to Eq. (6) is a boundary of stability. Below this line, the motion of the particle is unstable. The condition of Eq. (8) is described by the upper border line of the shaded area, which we defined by the requirement that the expression on the left hand side of Eq. (8) exceeds the expression on the right hand side by a factor of 100. Below this upper border line, the stationary motion of the particle is restricted by z values of the displacement much less than z_0. Above this upper boundary, the stationary motion is still possible; however, as our simulations have shown, the magnitude of the oscillations increases with frequency until at some value of frequency, exceeding the value on the upper border line by three to four times, the motion becomes unstable.

The diagrams of Figs. 3 and 4 are complimentary: The first of them allows to assess the stability region, when the viscous force should be taken into account, and the second one shows the limitation imposed by the gravitational force. When a particle is trapped, the compensation for the gravitational force is achieved by a phase shift of the particle motion relative to the ac potential.[23] In this case, the particle spends more time in the region with a higher field creating an average force counteracting the force of gravity.

D. Simulation of a particle motion in the trap

We calculated the particle motion for the following parameters: The potential of the particle $V=500$ V (the total charge on the particle is about $q\approx1.6\times10^{-12}$ C$=10^7e$, where e denotes the elementary charge), the particle diameter of 58 μm, the density $\rho_m\approx2$ g/cm^2, the mass of the particle $m\approx2\times10^{-7}$ g, the charge/mass ratio $q/m=0.008$ C/kg, the initial displacement is zero, the initial velocity $v_{x0}=v_{z0}=0$, $v_{y0}=5$ cm/s, $V_{ac}=500$ V, the frequency of the ac field $f=100$ Hz, $q_x=0.81$, and $h=0.014$. The calculations were performed for three values of the parameter of the viscous force, $p=0.038$, 0.076, and 0.76; the value $p=0.076$ corresponds to the normal atmospheric pressure of the air. The charged particle experiences damped oscillations approaching the equilibrium position (Fig. 5). For the y axis, the equilibrium corresponds to the center of the trap and the oscillations quickly reduce in magnitude; for the z axis, the equilibrium value is displaced due to gravity and the oscillations continue with a finite amplitude and a phase shift relative to the ac field [$\varphi=13°$ for conditions of Fig. 5(b)], which is necessary for the compensation of gravity. The simulations reveal the existence of an optimal value of the air viscosity, for which the particle has the fastest approach to the stationary state.

E. Experimental trapping of microparticles

The particles were picked up by a brush and then charged by rubbing the brush over the ring electrode of the trap. Some of the falling particles were then captured in the trap. By manipulating applied ac potential and frequency, the storage of one, two, and multiple particles of dipicolinic acid in a ring-type trap could be achieved, as is shown in Fig. 6. The dimensions of the trap are as indicated above; the typical parameters are $f=160$ Hz, $V_{ac}=800$ V, and $V_{dc}=0$, and the particle diameter is $d\approx30$-50 μm. The micromotion at the driving frequency caused vertical oscillations with typical amplitudes about few diameters of the particle that were observed in a microscope. The simulations according to Eqs. (4) confirm this observation. For conditions of the experiment and the particle potential $V=400$ V, the corresponding parameters $q_x\approx0.7$, $-a'_x\approx10^{-2}$, and $q/m\approx0.012$ C/kg are within the stable trapping regions on the diagrams of Figs. 3 and 4.

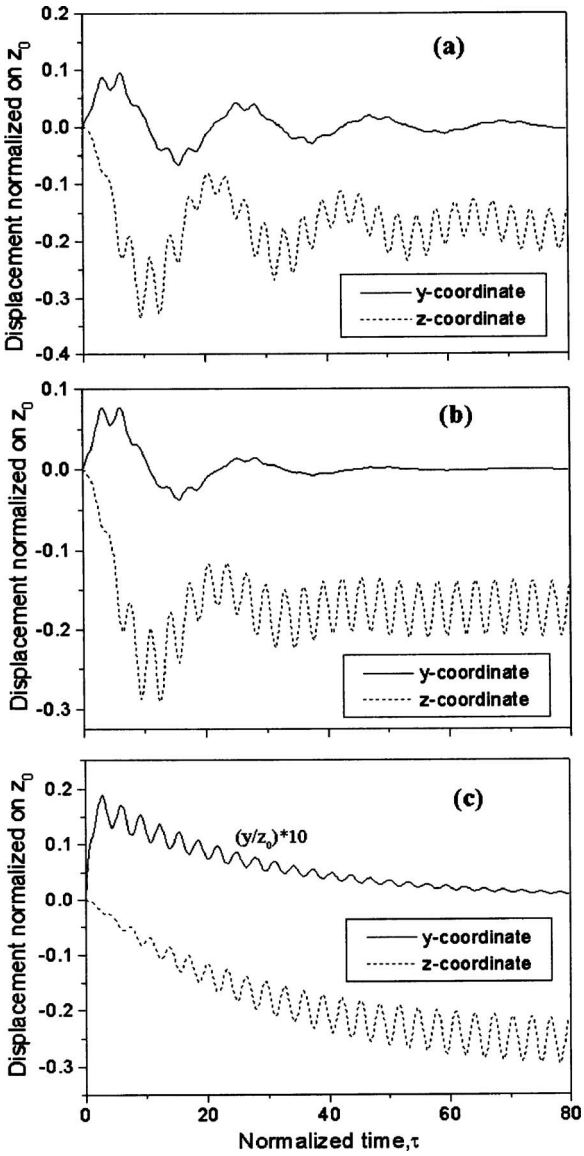

FIG. 5. Simulations of a particle motion in a ring-type trap for different values of the viscous parameter of the buffer gas: (a) $p=0.038$; (b) $p=0.076$; this value corresponds to the normal atmospheric pressure; and (c) $p=0.76$. The particle approaches the stationary state experiencing fast oscillations (micromotion) imposed on a larger-scale oscillations (macro or secular motion). The fastest approach to the stationary state is achieved at certain value of the viscous force [for the considered conditions, it corresponds to the air pressure close to normal, case (b)].

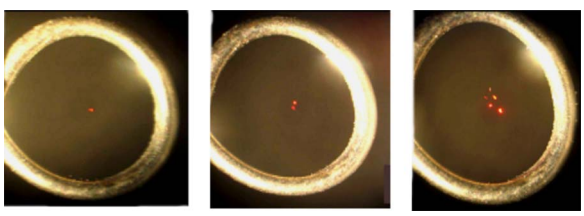

FIG. 6. (Color online) Storage of particles in a ring-type trap: One, two, and several particles. These dipicolinic acid particles are about 30–50 μm in size. For observation, they were illuminated by a He–Ne laser beam.

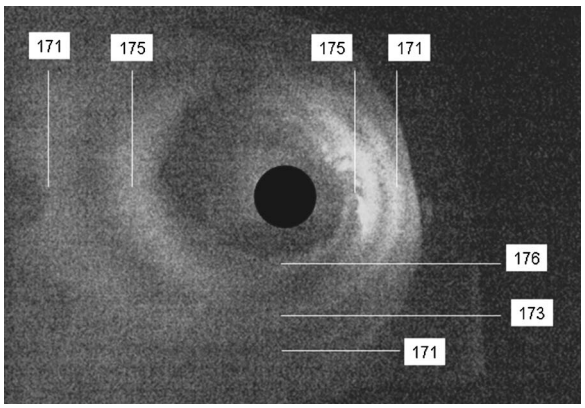

FIG. 7. The diffraction pattern of the backscattered light from a 9.6 μm particle. The numbers show the calculated angular positions (in degrees) of the bright circles in the backscattering relative to the incident beam.

IV. LIGHT SCATTERING ON TRAPPED MICROPARTICLES

A. Mie scattering

We studied scattering from both DPA particles and polystyrene particles suspended in our ring-type trap. Since DPA particles did not have a regular shape, their scattering pattern had a random, homogenized character. More characteristic patterns were exhibited by spherical polystyrene particles of 9.6 ± 1.9 μm diameter. The diameter of the particles substantially exceeded the optical wavelength, therefore, the scattered light intensity had well pronounced angular variations. This regular diffraction pattern characteristic of Mie scattering was registered (see Fig. 7) by a digital photo camera on a screen positioned at 45° to the backscattered light, as shown in Fig. 1(a).

B. Results of the Raman spectral measurements

A typical Raman spectrum measured with a DPA particle levitated in the trap is shown in Fig. 8. This spectrum was renormalized taking into account the transmission of the filter. The peaks observed in the Raman spectra correspond to characteristic vibrational modes of the DPA molecule. The

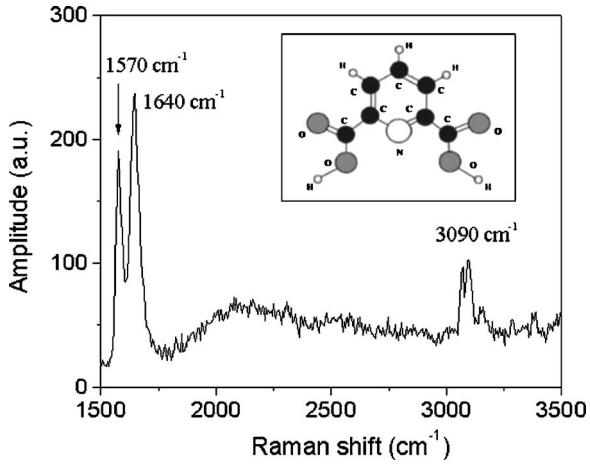

FIG. 8. Raman spectrum corrected for the filter transmission of a single DPA microparticle stored in the electrodynamic trap. The insert shows the structure of the DPA molecule.

identification of the peaks was done previously.[31,32] The three observed bands are a ring stretch (1570 cm^{-1}), C=O stretch (1640 cm^{-1}), and C–H stretch bands (3090 cm^{-1}).

V. DISCUSSION AND CONCLUSIONS

The stable trapping of a particle is possible when the amplitude of the ac field, its frequency, as well as the charge and mass of the particle satisfy certain relations corresponding to stable regions on the diagrams of Figs. 3 and 4. The force of gravity can be compensated by the ac field; in this case, the particle experiences vertical oscillations at the ac field frequency, but with a shifted phase. It should be noted that, for a trapped particle, typical values of the charge/mass ratio are quite different than those for trapped atomic and molecular ions. For instance, for the borderline case of particle with $d=86\ \mu m$ shown in Fig. 4, $q_0/m \approx 3.5 \times 10^{-3}$ C/kg. This value is much smaller than the values typical for trapping ions. For instance, for a singly charged magnesium ion, the ratio $e/m \approx 4 \times 10^6$ C/kg is many orders of magnitude higher, which requires a much higher frequency of the trapping ac voltage (usually about several megahertz).[3] For small particles, such as nanoparticles with diameter $d \approx 50$ nm, intermediate values of $q_0/m \approx 10^4$ C/kg can be expected, which require frequencies in the range of 0.1–1 MHz. The role of the viscous forces is also much higher for small particles at the same atmospheric pressure.

In a gas atmosphere, a charged particle can gradually lose its charge due to the interaction with the ions in the gas. The rate of the discharge is relatively slow (few elementary charges per second,[23] so that for most of the applications the storage time (on the order of an hour) is sufficiently long. If it is still necessary to extend the storage time, the particle can be trapped in vacuum.

We have described, numerically simulated, and observed storage of the microparticles in a simple Paul-Straubel ring-type trap. Such a trap provides an easy access for the laser beams to the stored species and is especially suited for scattering and spectroscopic studies of fine particles. We obtained the expression for the pseudopotential of such a trap, and the limits for confinement of charged particles were examined. Simulations of charged particles revealed the role of the gas (air) viscosity in the stabilization of the particle motion. The requirements for stable storage were analyzed and the stability diagrams in terms of the standard *a-q* parameters and the frequency-charge/mass ratio parameters were obtained. We studied the light scattering from microparticles stored in this simple trap, in particular, the diffraction patterns on 9.6 μm polystyrene particles were observed. The Raman spectrum of a single dipicolinic acid microparticle was measured using excitation at 488 nm and detection with a fiber optics spectrometer. For improving the collection of light, the trap with the stored particle was placed inside an elliptical mirror. The Raman spectra of a single DPA particle with a size about 50 μm could be measured with this arrangement. Using electrodynamic levitation allows to minimize the influence of the environment on the measurements. Avoiding the necessity for a substrate to support the sample by using an electrodynamic trap can be of advantage, for instance, for measurements on nanoparticles with extreme ultraviolet radiation that has high absorption in most of materials.

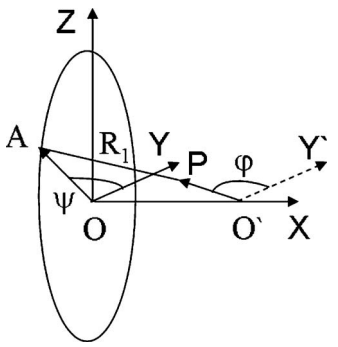

FIG. 9. The geometry of the problem for calculation of electric forces: O is the center of the ring trap, $P\{x,y,z\}$ is the position of the particle, $O'Y'$ is parallel to the axis OY, $OO'=x$, $OA=r_1$, and $OP=r$. The integration is performed over all points A on the ring.

ACKNOWLEDGMENTS

This work was partially supported by the Robert A. Welch foundation (Grant No. A1546) and by the National Science Foundation (Grant No. 0218595). Stimulating discussions with G. Kattawar are gratefully acknowledged.

APPENDIX: ELECTRIC FORCES FOR A RING-TYPE TRAP

The geometry of the problem determining the electric force acting on the particle is shown in Fig. 9. The frequency is assumed to be relatively low, so that the quasistatic approximation can be used. The components of the electric force on a charge q_0 placed at point $P\{x,\boldsymbol{r}\}$, where $\boldsymbol{r}=\{y,z\}=\{r\cos\varphi, r\sin\varphi\}$, is determined by the integrals of the contributions of the charges from all points $A\{x_1=0,\boldsymbol{r}_1\}$, with $\mathbf{r}_1=\{y_1,z_1\}=\{r_1\cos\psi, r_1\sin\psi\}$, along the ring,

$$F_x = q_0 E_x = q_0 \oint_C \frac{k\rho x}{R_1^3} r_1 d\psi,$$

$$F_y = q_0 E_z = q_0 \oint_C \frac{k\rho(r\cos\varphi - r_1\cos\psi)}{R_1^3} r_1 d\psi, \qquad \text{(A1)}$$

$$F_z = q_0 E_z = q_0 \oint_C \frac{k\rho(r\sin\varphi - r_1\sin\psi)}{R_1^3} r_1 d\psi,$$

where the integration loop C coincides with the ring of the trap (we approximate it by an infinitely thin line), ρ is the linear charge density of the ring, $R_1=(x^2+|\boldsymbol{r}_1-\boldsymbol{r}|^2)^{0.5}$, and $k=1/(4\pi\varepsilon\varepsilon_0)$, where ε_0 is the dielectric permittivity of vacuum and for the gas we assume $\varepsilon=1$.

Calculation of the above integrals in the assumption $r_1 \gg r$ gives the following result:

$$F_x = \frac{2\pi q_0 k \rho r_1}{R_1^3} x, \quad F_y = -\frac{\pi q_0 k \rho r_1}{R_1^5}(r_1^2 - 2x^2)y,$$
$$F_z = -\frac{\pi q_0 k \rho r_1}{R_1^5}(r_1^2 - 2x^2)z, \tag{A2}$$

where $R_1 = (x^2 + r_1^2)^{0.5}$. Assuming now that $r_1 \gg |x|$ and the radius of the ring to be much larger than the radius of the wire, i.e., $r_1 \gg r_w$, we obtain the amplitude of the oscillations of the linear charge density $\rho_m = V_{ac}/[2k \ln(r_1/r_w)]$ and also Eqs. (2). We would like to note that the field outside the central region of the trap can be presented as a series with Legendre polynomials,[33] and the solution for the electric potential at any value of the ratio r_1/r_w can be found using torroidal coordinates.[19]

[1] W. Paul and H. Steinwedel, Z. Naturforsch. A **8A**, 448 (1953).
[2] W. Paul and M. Z. Raether, Z. Phys. **140**, 262 (1955).
[3] H. G. Dehmelt, Adv. At. Mol. Phys. **3**, 53 (1967).
[4] H. Z. Straubel, Z. Elektrochem. **60**, 1033 (1956).
[5] R. A. Millikan, *Electrons (+ and −), Photons, Neutrons, and Cosmic Rays* (University of Chicago Press, Chicago, 1935).
[6] N. Yu, W. Nagourney, and H. Dehmelt, J. Appl. Phys. **69**, 3779 (1991).
[7] R. G. Brewer, R. G. DeVoe, and R. Kallenbach, Phys. Rev. A **46**, R6781 (1992).
[8] P. H. Kaye, Meas. Sci. Technol. **9**, 141 (1998).
[9] Y.-R. Chang, L. Hsu, and S. Chi, Opt. Commun. **246**, 97 (2005).
[10] J. Musick, J. Popp, and W. Kiefer, J. Mol. Struct. **480/481**, 317 (1999).
[11] J. W. Schweizer and D. N. Hanson, J. Colloid Interface Sci. **35**, 417 (1971).
[12] C. B. Richardson, A. L. Pigg, and R. L. Hightower, Proc. R. Soc. London, Ser. A **422**, 319 (1989).
[13] D. Duft, T. Achtzehn, R. Mueller, B. A. Huber, and T. Leisner, Nature (London) **421**, 128 (2003); T. Achtzehn, R. Müller, D. Duft, and T. Leisner, Eur. Phys. J. D **34**, 311 (2005).
[14] A. Ashkin, J. M. Dziedzic, J. E. Bjorkholm, and S. Chu, Opt. Lett. **11**, 288 (1986).
[15] R. F. Wuerker, H. Shelton, and R. V. Langmuir, J. Appl. Phys. **30**, 342 (1959).
[16] D. R. Secker, P. H. Kaye, and E. Hirst, Opt. Express **8**, 290 (2001).
[17] K. Ajito and K. Torimitsu, TrAC, Trends Anal. Chem. **20**, 255 (2001).
[18] W. Kiefer, J. Popp, M. Lankers, M. Trunk, I. Hartmann, E. Urlaub, and J. Musick, J. Mol. Struct. **408/409**, 113 (1997).
[19] N. Yu and W. Nagourney, J. Appl. Phys. **77**, 3623 (1995).
[20] R. A. Millikan, Phys. Rev. **22**, 1 (1923).
[21] B. E. Dahneke, J. Aerosol Sci. **4**, 139 (1971).
[22] K. C. Lea and S. K. Loyalka, Phys. Fluids **25**, 1550 (1982).
[23] R. H. Frickel, R. E. Shaffer, and J. B. Stamatoff, Chemical Systems Laboratory Report No. ARCSL-TR-77041, 1978.
[24] E. J. Davis and R. Periasamy, Langmuir **1**, 373 (1985).
[25] E. J. Davis, Aerosol Sci. Technol. **26**, 212 (1997).
[26] N. W. McLachlan, *Theory and Application of Mathieu Functions* (Clarendon, Oxford, 1947).
[27] G. Göebel, Th. Wriedt, and K. Bauckhage, Rev. Sci. Instrum. **68**, 3046 (1997).
[28] *The Bacterial Spore*, edited by G. W. Gould and A. Hurst (Academic, London, 1969).
[29] P. L. Kapitsa, Zh. Eksp. Teor. Fiz. **21**, 588 (1951).
[30] R. F. Wuerker, H. Shelton, and R. V. Langmuir, J. Appl. Phys. **30**, 342 (1959).
[31] P. Carmona, Spectrochim. Acta, Part A **36**, 705 (1980).
[32] A. A. Kolomenskii and H. A. Schuessler, Spectrochim. Acta, Part A **61**, 647 (2005).
[33] J. D. Jackson, *Classical Electrodynamics*, 2nd ed. (Wiley, New York, 1975); R. G. Brewer, R. G. DeVoe, and R. Kallenbach, Phys. Rev. A **46**, R6781 (1992).